



Intrarenal Pressure, Fluid Management, and Hydrodynamic Stone Retrieval in Mini-PCNL

14

Theodoros Tokas  and Udo Nagele

14.1 Introduction

Mini-PCNL (mPCNL) constitutes an advancing field in active renal stone treatment. Manufacturers have enriched our armamentarium with a variety of instruments. At the same time, different study groups have presented new techniques in patient body positioning, kidney puncture, and stone lithotripsy. Nevertheless, by decreasing instrument caliber to prevent damage caused by instrument access to the kidney, the water inflow–outflow balance is compromised. To achieve better visibility and improve stone clearance, the surgeon must increase irrigation flow (IF). This action results in an increase of inflow/irrigation pressures (IPs). However, subsequent intraoperative intrarenal pressure (IRP) increments can lead to serious complications [1]. This problem becomes more evident when utilizing extra-small instruments. Nonetheless, the majority of endourologists are not aware of normal and pathological IRP ranges during mini-PCNL and their impact on kidney physiology. In this chapter, we will present ways to maintain optimal fluid management to effectively remove stone fragments after lithotripsy and achieve perfect vision during

the whole procedure. Furthermore, we are going to discuss the influence of increased IRPs in complication development and prevention measures to control IRPs and, at the same time, maintain optimal irrigation flow.

14.2 Adverse Events Due to Increased IRPs

14.2.1 Fluid Backflow and Absorption (Fig. 14.1)

Pyelorenal backflow occurs when pelvic or calyceal fluid leaks into the sinus peripelvic tissue (pyelosinus backflow), the collecting ducts and tubules (pyelotubular backflow), the renal interstitium (pyelointerstitial backflow), or the renal vein (pyelointerstitial backflow) (pyelovenous backflow). Animal studies have presented that it occurs at pressures 40.8–47.6 cmH₂O [2]. Backflow to the renal vein may complicate even low pressures (13.6–27.2 cmH₂O) [3, 4] and becomes evident at 40.8–68 cmH₂O [5, 6]. At IRPs of 81.6–95.2 cmH₂O, different research groups have found a risk of pyelosinus backflow or even fornix rupture in rabbits [7, 8] and at 272 cmH₂O in pigs [9]. Irrigating fluid may reach the retroperitoneum in considerable amounts after renal pelvic perforation [10]. Low urine flow, vesicoureteral reflux, ischemic damage are possible pre-existing conditions that can lower

T. Tokas (✉) · U. Nagele
Department of Urology and Andrology, General
Hospital Hall in Tirol, Hall in Tirol, Austria
Training and Research in Urological Surgery and
Technology (T.R.U.S.T.)-Group, Hall in Tirol, Austria
e-mail: udo.nagele@tirol-kliniken.at



Fig. 14.1 Backflow and fluid absorption during PCNL demonstrated in a postoperative CT excretory phase

the backflow threshold [7, 11]. The direct intravascular absorption via opened veins, or the intraperitoneal space opening with subsequent peritoneal resorption, lead to the so-called “acute absorption syndrome” [3, 12]. Additional venous hemorrhage and renal pelvis wall lesions are possible contributing factors. Fluid absorption can occur directly into the opened veins or indirectly as a result of a perinephric irrigating fluid accumulation [13]. Reported fluid absorption during conventional PCNL ranges 50–2200 ml [3, 14, 15], but no data exist regarding miniaturized instruments.

14.2.2 Infections

Increased IRP, backflow, and urinary tract infections, fever, systemic inflammatory response syndrome (SIRS), and sepsis all have a direct link, demonstrating antibiotics’ beneficial effect. The amount of irrigation fluid used is also a potential

risk factor for SIRS [16]. In general, postoperative fever after PCNL appears in 10.8% of the cases [17]. Despite its low incidence rates (0.3–1%), septic shock is associated with significant mortality rates (66–80%) [18]. In addition, increments in IRP are a substantial risk factor for postoperative fever and urosepsis [19]. Finally, elevated IPs (272 cmH₂O) trigger SIRS more frequently (46%) than low IPs (108.8 cmH₂O/11%) [20]. However, information on the occurrence of infections following mini-PCNL is limited.

14.2.3 Kidney Damage

Animal studies have proven the direct correlation of increased IRP with irreversible damage [6, 21]. Immensely increased IPs (>200 cmH₂O) more probably have a detrimental effect on porcine kidneys in comparison with IPs less than 120 cmH₂O. An IRP as high as 250 cmH₂O can lead to a rupture of the collecting system [21]. Furthermore, pyeloinous backflow caused by fornical rupture can be the cause of perirenal pseudocysts, edema and hemorrhage of the retroperitoneum, perinephric abscess, and fibrolipomatosis [6]. Moreover, increased IRPs might lead to congestion due to calyceal urothelium denudation, and submucosal edema formation [6, 21]. Even 4–6 weeks following a procedure, tubular vacuolization, and degeneration, as well as pericalyceal vasculitis and metaplasia, have been observed [6, 21].

Due to microvessel compression and insufficient venous flow, high IRPs can cause oxidative damage to the kidney and subsequent loss of renal function. Of note, due to ischemia/reperfusion injury, venous outflow obstruction is more harmful than arterial obstruction [22, 23]. Pyelovenous backflow causes venous stagnation to some extent, resulting in perfusion pressure compression of microvessels, reducing the blood supply to the renal parenchyma. The resulting condition may be a renal ischemia, or reperfusion damage [24].

14.2.4 Various Complications

Urine leakage is a powerful fibrotic response causative factor [6, 25]. Furthermore, intrarenal backflow may cause papillary damage and consequent pathological stone growth development [26]. Due to fornix or parenchymal rupture, high IRPs can cause subcapsular hematomas [27] and potentially life-threatening perirenal bleedings [28]. The increase of the mean systolic and diastolic blood pressures might be considerable. Moreover, due to large elevations in renin, aldosterone, and ACTH levels, a propensity to hyponatremia and metabolic acidosis occurs. These alterations could be attributed to the invasive nature of kidney intervention and continuous irrigation, which has been linked to an increase in IRPs [29, 30].

14.2.5 Role of Time

Procedure times independently correlate with postoperative fever and SIRS rates [31, 32]. Additionally, infection risk and postoperative fever rates increase when IRPs remain higher than 40 cmH₂O for more than 10 min [33]. In pig models, renal cellular injury occurs within 1 h at IRPs of 20 cmH₂O or higher [34]. The volume of fluid absorbed during PCNL increases as the IRPs and procedure times increase [3]. After a total irrigation period of 30 min, fluid absorption reaches its peak. The volumes of absorbed irrigant after 30 and 90 min are 154 and 1360 ml, respectively [14]. From the 30th to the 120th irrigation minute, potassium levels drop and do not recover until 24 h after surgery. Researchers discovered an increase in Cl levels at the 120th minute of irrigation, as well as a lowering trend in pH from the beginning to the 120th minute of irrigation, which abates 24 h after surgery [15]. As a result of the prolonged irrigation durations, a trend toward metabolic acidosis can be seen. As a result, based on existing evidence, the total process time should not exceed 2 h [15].

14.2.6 Kidney Injury: The Role of Obstruction, Irrigation Pressure, and Irrigation Volume

Renal obstruction is detrimental because IPs starting at 82 cmH₂O are more likely to cause acute kidney damage in rats with substantially obstructed kidneys. Not obstructed kidneys, on the other hand, sustain no renal injuries, whereas partially obstructed kidneys sustain injuries only at pressures of 136 cmH₂O [35]. When rabbits are exposed to renal perfusion pressures of more than 82 cmH₂O, severely obstructed kidneys are more sensitive to oxidative damage and mitochondrial injury than slightly obstructed kidneys. Both obstructed and non-obstructed kidneys are damaged by irrigation pressures of 136 cmH₂O [24]. Current research advises keeping perfusion pressure between 70 and 410 cmH₂O during endourological procedures to keep the IRP limit below 30 cmH₂O and avoid kidney injury [36, 37].

14.3 IRPs during Mini-PCNL

14.3.1 IRP Measurement

Using pressure transducers in animals and people, researchers were able to get precise intraluminal pressure readings in the renal pelvis and ureter [38–40]. The Pressure Flow (PPF)—or Whitaker test—was introduced by Robert H. Whitaker, who created the groundwork by establishing an antegrade pressure measurement of the upper urinary tract [41]. He first used this technique on children, with the goal of identifying obstruction as a cause of urinary tract dilatation [41, 42]. Normal IRPs range from 12 to 15 cmH₂O, whereas pressures greater than 20 cmH₂O indicate an obstruction. Intermediate values range from 15 to 20 cmH₂O [43]. Nowadays, surgeons are able to measure intraoperative IRPs by placing a special catheter either antegradely after a kidney puncture in a way

similar to the Whitaker test, or retrogradely after catheterizing the ureteral orifice [44].

14.3.2 IRP Values during Different Conditions

The flow of a fluid through a rigid tube is influenced by the pressure gradient between its ends, the fluid viscosity, the length, and the diameter of the tube, according to the Poiseuille equation ($dP = 8VgL/pR^4$; $V = FR$ through the tube, $g =$ fluid viscosity, $L =$ tube length, and $R =$ tube radius) [45, 46]. Additional parameters, including the difference between internal and exterior pressures, external compression, wall tension, and wall thickness, play an important part in a collapsible tube. The transmural pressure equals the tension per unit length over the radius, according to the Laplace equation. The pressure gradually climbs to a certain capacity during the early filling phase, indicating the upper urinary tract's natural elasticity. The rise of the curve is a proxy for the compliance of the pelvic wall [46].

The IRPs at low urine FRs are not higher than a few cmH_2O in a normal human kidney with no obstruction [47]. During diuresis, however, IRPs may exceed $27.2 \text{ cmH}_2\text{O}$. They range from 68 to $95 \text{ cmH}_2\text{O}$ in chronic kidney blockage, and as a result, the values fall until the kidney is no longer functional [2]. In hydronephrosis, mean basal IRPs of $12 \text{ cmH}_2\text{O}$ have been reported [48], and at flow rates $>10 \text{ mL/min}$, the pressure reaches obstructive levels [49, 50]. Of note, there is also direct relevance between changes in intravesical pressure and IRP changes. In hydronephrotic kidneys, bladder pressure at 50% capacity is $8.9 \pm 3.1 \text{ cmH}_2\text{O}$, whereas pelvic pressure is $20.8 \pm 2.1 \text{ cmH}_2\text{O}$, compared to $7.4 \pm 1.1 \text{ cmH}_2\text{O}$ in non-hydronephrotic kidneys [51]. To avoid further increases in IRPs, the urinary bladder should be continually drained during endourological treatments.

14.3.3 IRPs during Mini-PCNL

In humans, IRPs have been tested in the following mini-PCNL systems; 9.5 Fr, 12 Fr, 14 Fr,

16 Fr, and 18 Fr with scopes of 7.5–9.8 Fr [32, 52–55]. Additionally, one study group have tested IRPs during micro-PCNL (4.8 Fr) [56]. Irrigation pressures range from 40 to $340 \text{ cmH}_2\text{O}$, with flow rates ranging from 250 to 580 mL/min . Surgeons usually utilize gravity to achieve adequate irrigation flow. Usually, IRPs are remaining below the critical level of $40 \text{ cmH}_2\text{O}$, and reach $30 \text{ cmH}_2\text{O}$ in 14 Fr, $20 \text{ cmH}_2\text{O}$ in 16 Fr, and $15 \text{ cmH}_2\text{O}$ in 18 Fr. Maximal IRPs of $>40 \text{ cmH}_2\text{O}$ have been documented with 9.5 F and 14 F sheaths [53, 57].

14.3.4 IRPs in Supine Versus Prone Mini-PCNL

Limited data exist comparing the two techniques. However, by taking into account the Poiseuille equation ($dP = 8VgL/pR^4$;) we conclude that the generated IRPs are proportional to the length of the access sheath (L) and reversely proportional to the sheath radius (R). In prone PCNL, the instrument angle ranges from $+30^\circ$ to $+90^\circ$ which means that the sheath adds up $1520 \text{ cmH}_2\text{O}$ to the estimated IRP. On the other hand, in supine PCNL the instrument angle ranges from 0° to -45° , which sometimes reduces pressures until the collecting system collapses. Therefore, using a slightly longer access sheath during supine position with the absence of a collapsing system may result in increased IRPs. Further research is deemed necessary to support this hypothesis.

14.4 Clearance of Fragments and Maintaining Low IRPs by Taking Advantage of Different Hydrodynamic Effects

The big caliber of standard PCNL systems allows maintenance of IRPs below $40 \text{ cmH}_2\text{O}$ [56, 58–62]. However, irrigation backflow via the access sheath is not achievable with very small-caliber instruments (less than 10 Fr), resulting in a mismatch between in- and outflow. Due to mechanical problems, the open sheath designs of the first-generation miniaturized instruments (15–20 Fr) are sufficient for pressure control [63]. The

smaller instrument diameter of miniaturized instruments often results in an increase in the number and decrease in the size of stone fragments to be harvested. With an ever-increasing quantity of microscopic fragments or even dust, stone retrieval is shifting away from mechanical methods and toward hydrodynamic effects. There are numerous essential concepts of hydrodynamic-assisted fragment removal that are independent of access.

14.4.1 Passive Washout

It is the secondary natural removal of stones over a period of time, usually specified as one week, one month, or three months. It is commonly accomplished by using a Mono-J stent for a few days, a Double-J stent for a longer period, or even without any stenting postoperatively.

14.4.2 Active Washout

It could be used in a variety of ways [64–66]. Transporting fragments within the continuous irrigation backflow through the access sheath alongside the scope is one option. During Chinese mini-PCNL, the surgeon fills the collecting system with high pressure with the nephroscope and then quickly removes it, causing an immediate inversion of irrigation flow and pressure, leading in a spillage-like stone removal throughout the access sheath. The irrigation flow pushes stone particles down the ureter during micro-perc. Finally, during ultra-mini PCNL, the surgeon injects irrigation fluid with a syringe into an extra channel within the access sheath and washes off fragments through the main channel of the access sheath without any pressure peaks.

14.4.3 Ureteral Sheaths and Catheters

During conventional PCNL, the concept of a retrograde ureteral catheter or ureteral access sheath (UAS) placement was introduced [36]. When compared to an empty ureter (11–38 cmH₂O), a

ureteral catheter (15–52 cmH₂O), or an occlusion balloon application (16–56 cmH₂O), researchers found that using a 10/12 Fr or 12/14 Fr UAS (5–22 cmH₂O) resulted in lower IRPs. In the case of mPCNL, the inclusion of a suction device can help with the fluid washing out. In a cadaveric pork model, a combination of pressure irrigation with sensor-controlled suction using a modified transurethral 8-Fr mono-J catheter with expanded drainage holes resulted in enhanced irrigation flow and lower IRP [67].

Purging effect [67] is a pressure-controlled irrigation process that transports fragments through a percutaneous entry and outflows through a Mono-J catheter or UAS (Fig. 14.2). It provides a high irrigation fluid turnover as well as effective fragment transportation without causing pressure overload in the collecting system. This approach is particularly appealing for stone clearance in small-caliber percutaneous instruments, where adequate simultaneous in- and outflow irrigation via the same access is not usually possible due to construction and stability issues. IRPs could be reduced by 14% at 100 cmH₂O (19–14.5 cmH₂O) and 28% at 150 cmH₂O input pressure (37–26.5 cmH₂O) due to the purging action.

14.4.4 Vacuum Cleaner Effect (Fig. 14.3) [68]

In a cadaveric pork model, the minimally invasive PCNL (MIP) idea was initially tested using an 18 Fr nephroscope sheath with an open proximal end [63]. In low-pressure settings, the vacuum-cleaner effect is the active and purposeful entrapment of fragments in a hydrodynamic pseudo cavity in front of the scope. The effect resembles mechanical forceps, such as an invisible grasper, and it is not simply a washout phenomenon. It emerges when a slipstream forms in front of the distal end of a round-shaped nephroscope, which is caused by an excursive shift in the width of the fluid flow at the flushing canal's exit. It is determined by the relationship between the diameter of the nephroscope and the diameter of the inner sheath. The greatest benefit is obtained with a 12 Fr nephroscope and a 15 Fr

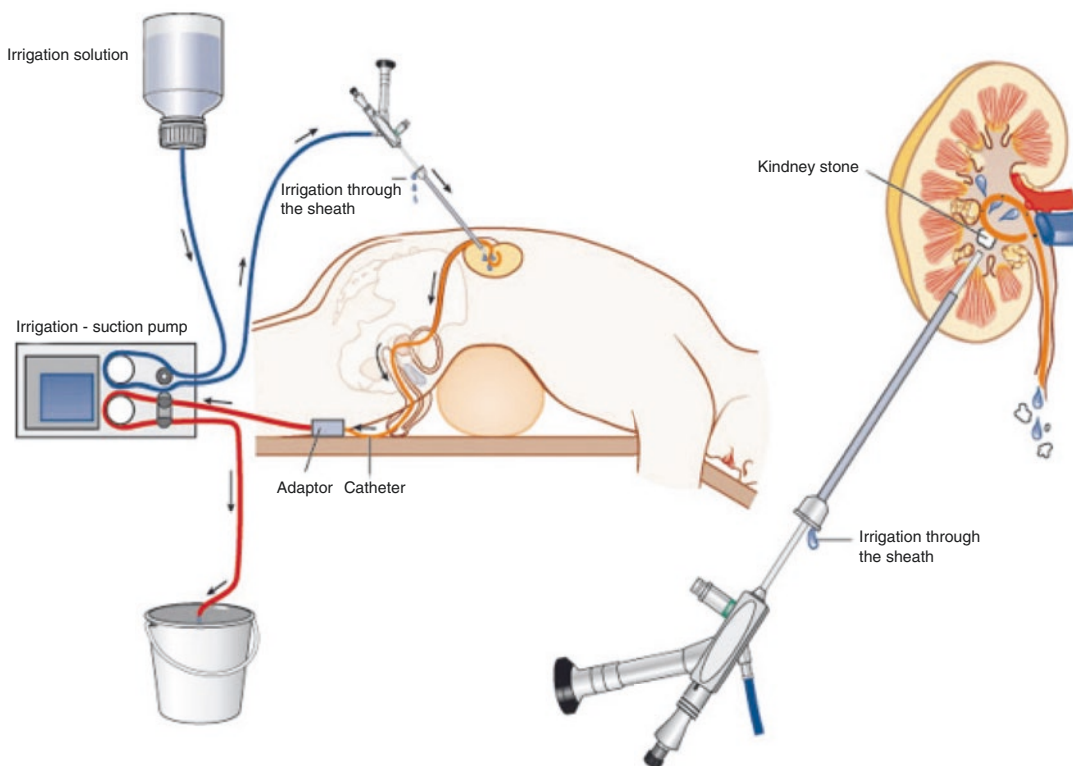


Fig. 14.2 The *purging effect* is the fragment transportation process by pressure-controlled irrigation using inflow through the percutaneous access and outflow through a Mono-J catheter or UAS

inner sheath diameter; however, utilizing a 16.5 Fr sheath with a 12 Fr scope creates an ideal combination (pressure/stone clearance) at the cost of a high IRP [68].

14.4.5 Pressure/Suction Connected with the Nephroscope

During mPCNL, Song et al. introduced a unique irrigation and clearance method (16 Fr). The irrigation volume was 600–800 mL/min, the irrigation pressure was 340–410 cmH₂O, and the suction pressure was 140–340 cmH₂O. The IRP remained below six cmH₂O on average [69]. Different settings included an irrigation volume of 600–800 mL/min, irrigation pressure of 340–410 cmH₂O, and suction pressure of 140–340 cmH₂O. IRPs remained below six cmH₂O. Yang et al. [70] demonstrated a mini-

PCNL (12 Fr) setup with intelligent monitoring and control of IRPs below three cmH₂O.

14.4.6 Stone Clearance in Small and Extrasmall Instruments (Ultraminiperc, Superperc, Super-Mini Perc, MIP S, MIP XS)

The MIP S system (Karl Storz, Germany) is the smallest instrument with regular backflow via the access sheath in percutaneous surgery, and it was also the smallest percutaneous OR system to create a vacuum cleaner effect in a low-pressure setting [68]. Because irrigation backflow via access sheath was not possible due to the mechanical features of the instruments, all smaller systems, such as the Microperc (Polydiagnost, Germany) and the MIP XS system by Nagele (Karl Storz,

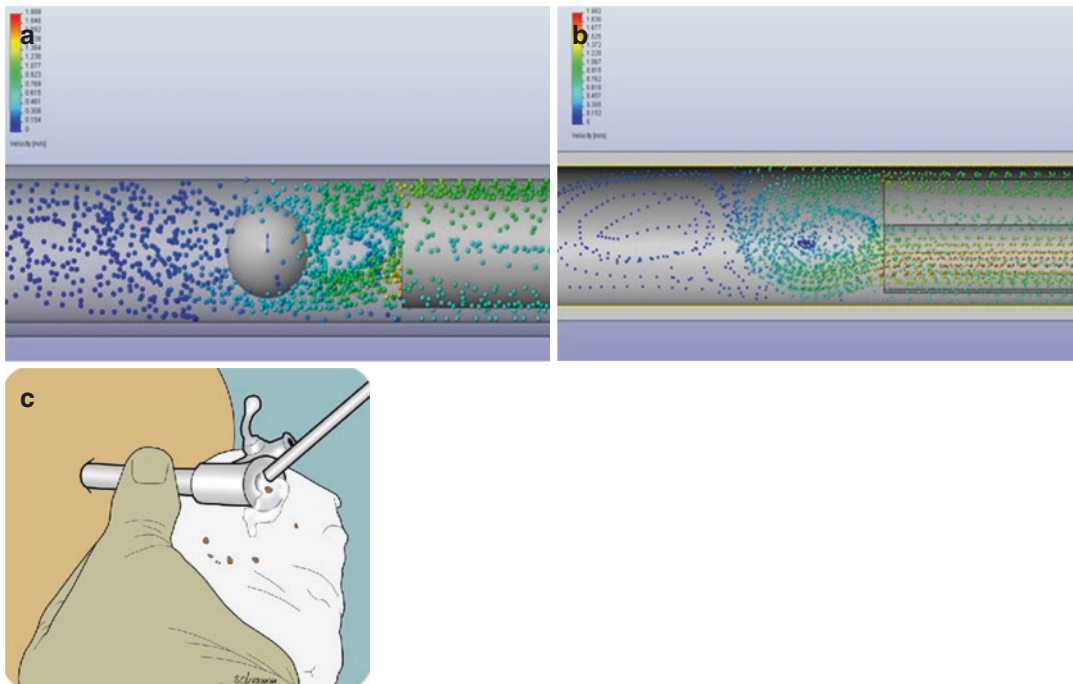


Fig. 14.3 Vacuum cleaner effect. In front of the distal end of the round-shaped nephroscope a slipstream is developing induced by the excursive change of width of the fluid flow on the outlet of the flushing canal (a). This allows the

adhesion of a stone fragment in the eddy while the fluid flow is circulating around the stone (b). By pulling the scope through the sheath the stones are spontaneously evacuated through the proximal end (c)

Germany), rely on an outflow utilizing a ureteric catheter. The MIP XS system uses a sensor-controlled dual action pump with purging effect and active pressure control, whereas the Microperc system depends on both active and passive washout without pressure control.

The ultraminiperc uses a 13-Fr access sheath and a 3.5-Fr nephroscope in a 6-Fr inner sheath as a final step in downsizing (Schoelly Fiberoptics GmbH, Denzlingen, Germany) [64]. MIP 2.0, a MIP set expansion by Nagele, is now available in sizes “S” and “X.S.” with access sheath diameters of 8.5/9.5 and 11/12 Fr and a nephroscope diameter of 7.5 Fr (Karl Storz GmbH). The isotonic saline can flow beside the inner sheath through the outer sheath due to the unique construction of these instruments [64]. However, this effect can only be achieved with an 11/12 Fr sheath, not an 8.5/9.5 sheath. Following the removal of the inner sheath with the nephroscope during ultraminiperc, the surgeon flushes stone fragments by injecting saline through the integrated channel

inside the sheath with a syringe, causing a jet in the calyx and the stones to escape, resulting in the so-called whirlpool effect [64, 71].

The super-miniperc (8 Fr scope, 12 Fr or 14 Fr double-layer metal sheath) [54, 55], superperc (4.5/6 Fr scope, 10/12 Fr sheath, Richard Wolf) [72] and ClearPetra (12 Fr scope, 16 Ch disposable sheath, Well Lead Medical Co., Ltd., China) [73] systems achieve a stone clearance depending on an irrigation-suction mechanism. Stone fragments are removed through an additional tube connected to a negative pressure aspirator.

All currently available small and extra small-caliber instruments offer attractive options in the armamentarium of modern percutaneous stone surgery. Nevertheless, the absence of high-quality data limits their wide distribution and implementation in the everyday clinical praxis. Furthermore, all hydrodynamic benefits are also applicable in conventional modern PCNL instruments, which leads to the term minimally invasive PCNL (MIP) [63, 68].

References

1. Tokas T, Herrmann TRW, Skolarikos A, Nagele U. Pressure matters: intrarenal pressures during normal and pathological conditions, and impact of increased values to renal physiology. *World J Urol.* 2018; <https://doi.org/10.1007/s00345-018-2378-4>.
2. Hinman F, Redewill FH. Pyelovenous back flow. *J Am Med Assoc.* 1926;87(16):1287–93. <https://doi.org/10.1001/jama.1926.02680160035011>.
3. Kukreja RA, Desai MR, Sabnis RB, Patel SH. Fluid absorption during percutaneous nephrolithotomy: does it matter? *J Endourol.* 2002;16(4):221–4. <https://doi.org/10.1089/089277902753752160>.
4. Stenberg A, Bohman SO, Morsing P, Muller-Suur C, Olsen L, Persson AE. Back-leak of pelvic urine to the bloodstream. *Acta Physiol Scand.* 1988;134(2):223–34. <https://doi.org/10.1111/j.1748-1716.1988.tb08483.x>.
5. Boccafoschi C, Lugnani F. Intra-renal reflux. *Urol Res.* 1985;13(5):253–8.
6. Jung HU, Frimodt-Moller PC, Osther PJ, Mortensen J. Pharmacological effect on pyeloureteric dynamics with a clinical perspective: a review of the literature. *Urol Res.* 2006;34(6):341–50. <https://doi.org/10.1007/s00240-006-0069-x>.
7. Thomsen HS, Dorph S, Olsen S. Pyelorenal backflow in normal and ischemic rabbit kidneys. *Investig Radiol.* 1981;16(3):206–14.
8. Thomsen HS, Dorph S, Olsen S. Pyelorenal backflow in rabbits following clamping of the renal vein and artery: radiologic and microscopic investigation. *Acta Radiol Diagn.* 1982;23(2):143–8.
9. Thomsen HS, Larsen S, Talner LB. Pyelorenal backflow during retrograde pyelography in normal and ischemic porcine kidneys. A radiologic and pathoanatomic study. *Eur Urol.* 1982;8(5):291–7.
10. Carson CC, Nesbitt JA. Peritoneal extravasation during percutaneous lithotripsy. *J Urol.* 1985;134(4):725–7.
11. Hodson CJ. The effects of disturbance of flow on the kidney. *J Infect Dis.* 1969;120(1):54–60.
12. Sinclair JF, Hutchison A, Baraza R, Telfer AB. Absorption of 1.5% glycine after percutaneous ultrasonic lithotripsy for renal stone disease. *Br Med J (Clin Res Ed).* 1985;291(6497):691–2.
13. Dimberg M, Norlen H, Hoglund N, Allgen LG. Absorption of irrigating fluid during percutaneous transrenal lithotripsy. *Scand J Urol Nephrol.* 1993;27(4):463–7.
14. Malhotra SK, Khaitan A, Goswami AK, Gill KD, Dutta A. Monitoring of irrigation fluid absorption during percutaneous nephrolithotripsy: the use of 1% ethanol as a marker. *Anaesthesia.* 2001;56(11):1103–6.
15. Xu S, Shi H, Zhu J, Wang Y, Cao Y, Li K, Wang Y, Sun Z, Xia S. A prospective comparative study of haemodynamic, electrolyte, and metabolic changes during percutaneous nephrolithotomy and minimally invasive percutaneous nephrolithotomy. *World J Urol.* 2014;32(5):1275–80. <https://doi.org/10.1007/s00345-013-1204-2>.
16. Zhong W, Leto G, Wang L, Zeng G. Systemic inflammatory response syndrome after flexible ureteroscopic lithotripsy: a study of risk factors. *J Endourol.* 2015;29(1):25–8. <https://doi.org/10.1089/end.2014.0409>.
17. Seitz C, Desai M, Hacker A, Hakenberg OW, Liatsikos E, Nagele U, Tolley D. Incidence, prevention, and management of complications following percutaneous nephrolitholapaxy. *Eur Urol.* 2012;61(1):146–58. <https://doi.org/10.1016/j.eururo.2011.09.016>.
18. Michel MS, Trojan L, Rassweiler JJ. Complications in percutaneous nephrolithotomy. *Eur Urol.* 2007;51(4):899–906. discussion 906. <https://doi.org/10.1016/j.eururo.2006.10.020>.
19. Kreydin EI, Eisner BH. Risk factors for sepsis after percutaneous renal stone surgery. *Nat Rev Urol.* 2013;10(10):598–605. <https://doi.org/10.1038/nrurol.2013.183>.
20. Omar M, Noble M, Sivalingam S, El Mahdy A, Gamal A, Farag M, Monga M. Systemic inflammatory response syndrome after percutaneous nephrolithotomy: a randomized single-blind clinical trial evaluating the impact of irrigation pressure. *J Urol.* 2016;196(1):109–14. <https://doi.org/10.1016/j.juro.2016.01.104>.
21. Schwalb DM, Eshghi M, Davidian M, Franco I. Morphological and physiological changes in the urinary tract associated with ureteral dilation and ureteropyeloscopy: an experimental study. *J Urol.* 1993;149(6):1576–85.
22. Li X, Liu M, Bedja D, Thoburn C, Gabrielson K, Racusen L, Rabb H. Acute renal venous obstruction is more detrimental to the kidney than arterial occlusion: implication for murine models of acute kidney injury. *Am J Physiol Renal Physiol.* 2012;302(5):F519–25. <https://doi.org/10.1152/ajprenal.00011.2011>.
23. Park Y, Hirose R, Dang K, Xu F, Behrends M, Tan V, Roberts JP, Niemann CU. Increased severity of renal ischemia-reperfusion injury with venous clamping compared to arterial clamping in a rat model. *Surgery.* 2008;143(2):243–51. <https://doi.org/10.1016/j.surg.2007.07.041>.
24. Cao Z, Yu W, Li W, Cheng F, Rao T, Yao X, Zhang X, Larre S. Oxidative damage and mitochondrial injuries are induced by various irrigation pressures in rabbit models of mild and severe hydronephrosis. *PLoS One.* 2015;10(6):e0127143. <https://doi.org/10.1371/journal.pone.0127143>.
25. Hodson CJ. Neuhauser lecture. Reflux nephropathy: a personal historical review. *AJR Am J Roentgenol.* 1981;137(3):451–62. <https://doi.org/10.2214/ajr.137.3.451>.
26. Thomsen HS. Pyelorenal backflow. Clinical and experimental investigations. Radiologic, nuclear, medical and pathoanatomic studies. *Dan Med Bull.* 1984;31(6):438–57.
27. Meng H, Chen S, Chen G, Tan F, Wang C, Shen B. Renal subcapsular hemorrhage complicating

- ureterolithotripsy: an unknown complication of a known day-to-day procedure. *Urol Int.* 2013;91(3):335–9. <https://doi.org/10.1159/000350891>.
28. Xu L, Li G. Life-threatening subcapsular renal hematoma after flexible ureteroscopic laser lithotripsy: treatment with superselective renal arterial embolization. *Urolithiasis.* 2013;41(5):449–51. <https://doi.org/10.1007/s00240-013-0585-4>.
 29. Atici S, Zeren S, Aribogani A. Hormonal and hemodynamic changes during percutaneous nephrolithotomy. *Int Urol Nephrol.* 2001;32(3):311–4.
 30. Mohta M, Bhagchandani T, Tyagi A, Pendse M, Sethi AK. Haemodynamic, electrolyte and metabolic changes during percutaneous nephrolithotomy. *Int Urol Nephrol.* 2008;40(2):477–82. <https://doi.org/10.1007/s11255-006-9093-6>.
 31. Dogan HS, Sahin A, Cetinkaya Y, Akdogan B, Ozden E, Kendi S. Antibiotic prophylaxis in percutaneous nephrolithotomy: prospective study in 81 patients. *J Endourol.* 2002;16(9):649–53. <https://doi.org/10.1089/089277902761402989>.
 32. Zhong W, Zeng G, Wu K, Li X, Chen W, Yang H. Does a smaller tract in percutaneous nephrolithotomy contribute to high renal pelvic pressure and postoperative fever? *J Endourol.* 2008;22(9):2147–51. <https://doi.org/10.1089/end.2008.0001>.
 33. Guo HQ, Shi HL, Li XG, Gan WD, Zeng LQ, Liu GX, Yang Y, Liu TS. [Relationship between the intrapelvic perfusion pressure in minimally invasive percutaneous nephrolithotomy and postoperative recovery]. *Zhonghua wai ke za zhi [Chinese J Surgery]*. 2008;46(1):52–4.
 34. Fung LC, Atala A. Constant elevation in renal pelvic pressure induces an increase in urinary N-acetyl-beta-D-glucosaminidase in a nonobstructive porcine model. *J Urol.* 1998;159(1):212–6.
 35. Cao Z, Yu W, Li W, Cheng F, Xia Y, Rao T, Yao X, Zhang X, Larre S. Acute kidney injuries induced by various irrigation pressures in rat models of mild and severe hydronephrosis. *Urology.* 2013;82(6):1453.e9–16. <https://doi.org/10.1016/j.urology.2013.08.024>.
 36. Landman J, Venkatesh R, Ragab M, Rehman J, Lee DI, Morrissey KG, Monga M, Sundaram CP. Comparison of intrarenal pressure and irrigant flow during percutaneous nephroscopy with an indwelling ureteral catheter, ureteral occlusion balloon, and ureteral access sheath. *Urology.* 2002;60(4):584–7.
 37. Shao Y, Shen ZJ, Zhu YY, Sun XW, Lu J, Xia SJ. Fluid-electrolyte and renal pelvic pressure changes during ureteroscopic lithotripsy. *Minim Invasive Ther Allied Technol.* 2012;21(4):302–6. <https://doi.org/10.3109/13645706.2011.595419>.
 38. Rattner WH, Fink S, Murphy JJ. Pressure studies in the human ureter and renal pelvis. *J Urol.* 1957;78(4):359–62.
 39. Struthers NW. The role of manometry in the investigation of pelvi-ureteral function. *Br J Urol.* 1969;41(2):129–62.
 40. Weaver RG, Yelderman JJ. The positive pressure catheter for measurement of intracavitary pressures and pressure patterns. *J Urol.* 1967;98(6):718–20.
 41. Whitaker RH. Methods of assessing obstruction in dilated ureters. *Br J Urol.* 1973;45(1):15–22.
 42. Whitaker RH. An evaluation of 170 diagnostic pressure flow studies of the upper urinary tract. *J Urol.* 1979;121(5):602–4.
 43. Veenboer PW, de Jong TP. Antegrade pressure measurement as a diagnostic tool in modern pediatric urology. *World J Urol.* 2011;29(6):737–41. <https://doi.org/10.1007/s00345-011-0717-9>.
 44. Doizi S, Letendre J, Cloutier J, Ploumidis A, Traxer O. Continuous monitoring of intrapelvic pressure during flexible ureteroscopy using a sensor wire: a pilot study. *World J Urol.* 2020; <https://doi.org/10.1007/s00345-020-03216-w>.
 45. Pfizner J. Poiseuille and his law. *Anaesthesia.* 1976;31(2):273–5.
 46. Bullock KN. The biomechanical principles of upper urinary tract pressure-flow studies. *Br J Urol.* 1983;55(2):136–9.
 47. Kiil F. Pressure recordings in the upper urinary tract. *Scand J Clin Lab Invest.* 1953;5(4):383–4. <https://doi.org/10.3109/00365515309094217>.
 48. Kinn AC. Pressure flow studies in hydronephrosis. *Scand J Urol Nephrol.* 1981;15(3):249–55.
 49. Lupton EW, Holden D, George NJ, Barnard RJ, Rickards D. Pressure changes in the dilated upper urinary tract on perfusion at varying flow rates. *Br J Urol.* 1985;57(6):622–4.
 50. Pfister RC, Newhouse JH, Hendren WH. Percutaneous pyeloureteral urodynamics. *Urol Clin North Am.* 1982;9(1):41–9.
 51. Fichtner J, Boineau FG, Lewy JE, Sibley RK, Vari RC, Shortliffe LM. Congenital unilateral hydronephrosis in a rat model: continuous renal pelvic and bladder pressures. *J Urol.* 1994;152(2 Pt 2):652–7.
 52. Guohua Z, Wen Z, Xun L, Wenzhong C, Yongzhong H, Zhaohui H, Ming L, Kaijun W. The influence of minimally invasive percutaneous nephrolithotomy on renal pelvic pressure in vivo. *Surg Laparosc Endosc Percutan Tech.* 2007;17(4):307–10. <https://doi.org/10.1097/SLE.0b013e31806e61f4>.
 53. Huusmann S, Wolters M, Schilling D, Kruck S, Bader M, Tokas T, Herrmann TR, Nagele U. [Pressure study of two miniaturised amplatz sheaths of 9.5 F and 12 F outer diameter for minimal invasive percutaneous nephrolithotomy (MIP): an ex vivo organ model measurement]. *Aktuelle Urol.* 2018. <https://doi.org/10.1055/a-0759-0140>.
 54. Zeng G, Zhu W, Liu Y, Fan J, Lam W, Lan Y, Cai C, Deng T, Li X, Zhao Z. Prospective comparative study of the efficacy and safety of new-generation versus first-generation system for super-mini-percutaneous nephrolithotomy: a revolutionary approach to improve endoscopic vision and stone removal. *J Endourol.* 2017;31(11):1157–63. <https://doi.org/10.1089/end.2017.0558>.

55. Zeng G, Zhu W, Liu Y, Fan J, Zhao Z, Cai C. The new generation super-mini percutaneous nephrolithotomy (SMP) system: a step-by-step guide. *BJU Int.* 2017;120(5):735–8. <https://doi.org/10.1111/bju.13955>.
56. Tepeler A, Akman T, Silay MS, Akcay M, Ersoz C, Kalkan S, Armagan A, Sarica K. Comparison of intrarenal pelvic pressure during micro-percutaneous nephrolithotomy and conventional percutaneous nephrolithotomy. *Urolithiasis.* 2014;42(3):275–9. <https://doi.org/10.1007/s00240-014-0646-3>.
57. Tokas T, Skolarikos A, Herrmann TRW, Nagele U. Pressure matters 2: intrarenal pressure ranges during upper-tract endourological procedures. *World J Urol.* 2018; <https://doi.org/10.1007/s00345-018-2379-3>.
58. Saltzman B, Khasidy LR, Smith AD. Measurement of renal pelvis pressures during endourologic procedures. *Urology.* 1987;30(5):472–4.
59. Goble NM, Hammonds JC. An in vitro study of intracavitary pressures during percutaneous nephrolithotomy. *Br J Urol.* 1987;60(4):307–11.
60. Low RK. Nephroscopy sheath characteristics and intrarenal pelvic pressure: human kidney model. *J Endourol.* 1999;13(3):205–8. <https://doi.org/10.1089/end.1999.13.205>.
61. Troxel SA, Low RK. Renal intrapelvic pressure during percutaneous nephrolithotomy and its correlation with the development of postoperative fever. *J Urol.* 2002;168(4 Pt 1):1348–51. <https://doi.org/10.1097/01.ju.0000030996.64339.fi>.
62. Mager R, Balzereit C, Reiter M, Gust K, Borgmann H, Husch T, Nagele U, Haferkamp A, Schilling D. Introducing a novel in vitro model to characterize hydrodynamic effects of percutaneous nephrolithotomy systems. *J Endourol.* 2015;29(8):929–32. <https://doi.org/10.1089/end.2014.0854>.
63. Nagele U, Horstmann M, Sievert KD, Kuczyk MA, Walcher U, Hennenlotter J, Stenzl A, Anastasiadis AG. A newly designed amplatiz sheath decreases intrapelvic irrigation pressure during mini-percutaneous nephrolitholapaxy: an in-vitro pressure-measurement and microscopic study. *J Endourol.* 2007;21(9):1113–6. <https://doi.org/10.1089/end.2006.0230>.
64. Desai J, Solanki R. Ultra-mini percutaneous nephrolithotomy (UMP): one more armamentarium. *BJU Int.* 2013;112(7):1046–9. <https://doi.org/10.1111/bju.12193>.
65. Desai MR, Sharma R, Mishra S, Sabnis RB, Stief C, Bader M. Single-step percutaneous nephrolithotomy (microperc): the initial clinical report. *J Urol.* 2011;186(1):140–5. <https://doi.org/10.1016/j.juro.2011.03.029>.
66. Li X, He Z, Wu K, Li SK, Zeng G, Yuan J, He Y, Lei M. Chinese minimally invasive percutaneous nephrolithotomy: the Guangzhou experience. *J Endourol.* 2009;23(10):1693–7. <https://doi.org/10.1089/end.2009.1537>.
67. Nagele U, Walcher U, Bader M, Herrmann T, Kruck S, Schilling D. Flow matters 2: how to improve irrigation flow in small-calibre percutaneous procedures—the purging effect. *World J Urol.* 2015; <https://doi.org/10.1007/s00345-015-1486-7>.
68. Nicklas AP, Schilling D, Bader MJ, Herrmann TR, Nagele U. The vacuum cleaner effect in minimally invasive percutaneous nephrolitholapaxy. *World J Urol.* 2015; <https://doi.org/10.1007/s00345-015-1541-4>.
69. Song L, Chen Z, Liu T, Zhong J, Qin W, Guo S, Peng Z, Hu M, Du C, Zhu L, Yao L, Yang Z, Huang J, Xie D. The application of a patented system to minimally invasive percutaneous nephrolithotomy. *J Endourol.* 2011;25(8):1281–6. <https://doi.org/10.1089/end.2011.0032>.
70. Yang Z, Song L, Xie D, Deng X, Zhu L, Fan D, Peng Z, Guo S, Ye Z. The new generation mini-PCNL system—monitoring and controlling of renal pelvic pressure by suctioning device for efficient and safe PCNL in managing renal staghorn calculi. *Urol Int.* 2016;97(1):61–6. <https://doi.org/10.1159/000442002>.
71. Nagele U, Nicklas A. Vacuum cleaner effect, purging effect, active and passive wash out: a new terminology in hydrodynamic stone retrieval is arising—does it affect our endourologic routine? *World J Urol.* 2016;34(1):143–4. <https://doi.org/10.1007/s00345-015-1575-7>.
72. Shah K, Agrawal MS, Mishra DK. Superperc: a new technique in minimally-invasive percutaneous nephrolithotomy. *Indian J Urol.* 2017;33(1):48–52. <https://doi.org/10.4103/0970-1591.194784>.
73. Zanetti SP, Lievore E, Fontana M, Turetti M, Gallioli A, Longo F, Albo G, De Lorenzis E, Montanari E. Vacuum-assisted mini-percutaneous nephrolithotomy: a new perspective in fragments clearance and intrarenal pressure control. *World J Urol.* 2020; <https://doi.org/10.1007/s00345-020-03318-5>.